Nuclear Instruments and Methods in Physics Research B 539 (2023) 136–140

Contents lists available at ScienceDirect

Nuclear Inst. and Methods in Physics Research, B

journal homepage: www.elsevier.com/locate/nimb

Proton beam induced degradation of Pioloform® (polyvinyl butyral (PVB)) support films used for analysis of biomedical tissue sections

Harry J. Whitlow [a,b,*], Gyula Nagy [c]

[a] Department of Physics, University of Oslo, Postboks 1048 Blindern, Oslo, N-0316, Norway
[b] Tandem Laboratory, Uppsala University, P.O. Box 529, Uppsala, SE-751 21, Sweden
[c] Department of Physics and Astronomy, Uppsala University, P.O. Box 516, Uppsala, SE-751 20, Sweden

ARTICLE INFO

Keywords:
Pioloform
Polyvinyl butyral (PVB)
MeV proton irradiation
Ion microprobe
Scanning Transmission Ion Microscopy (STIM)
Elastic Backscattering Spectrometry (EBS)

ABSTRACT

Pioloform®, an often used support film for ion microprobe research is a terpolymer of polyvinyl butyral (PVB) and $\lesssim$ 18 mass % polyvinyl alcohol (PVA). Simultaneous off-axis Scanning Transmission Ion Microscopy (OA-STIM) and Elastic Backscattering Spectrometry (EBS) measurements have been used to measure the evolution of the C, H and O contents for an increasing proton fluence. The results showed that the composition at zero proton-fluence was in close agreement with the theoretical atomic composition. This strongly suggests OA-STIM measurements. With increasing proton fluences preferential loss of H and O was observed from the films.

1. Introduction

Pioloform® is a commercial polymer that has been widely used as a support film in the analysis of tissue sections in MeV ion microprobes [1–6]. It can be formed as self-supporting thin film (0.3–2 μm) by coating on a flat substrate and transferred to a support by floating on deionised water. Pioloform is a random terpolymer that is largely comprised of polyvinyl butyral (PVB) units with 14–18 wt.% polyvinyl alcohol (PVA) and a lesser amount of polyvinyl acetate (PVa) units [7]. The structural formula presented in Fig. 1 shows that Pioloform only contains C, H and O giving it the advantage over e.g. Si_3N_4 membranes [8,9] that it does not contribute any heavy element signals to Particle Induced X-ray Emission (PIXE) spectra that could confound the analysis. Pioloform has a composition of 31.52 at.% C, 57.88 at.% H, 10.60 at.% O [7]. Furthermore, the H content only increases by 4.7 at.%, respectively when the content of PVA increases from 0 to 16 mass% [7]. This makes Pioloform support films interesting to use as an internal standard for determining the major element (H, C, N and O) contents when analysing biological tissue sections.

Previously, on- and off-axis Scanning Transmission Ion Microscopy (OA-STIM) has been employed to measure the thickness of biological samples [10–15]. This is unsatisfactory because the relative contents of the major elements C, H, N and O affect the mass density and more significantly the electron density. The latter governs the stopping force ($-dE/dx$) and the X-ray absorption coefficients which are important factors for quantitative analysis of PIXE data from lesser- and trace life-elements. Off-axis Scanning Transmission Ion Microscopy (OA-STIM) is conceptually similar to proton elastic scattering analysis (PESA) which has been used to determine the H-content of aerosol particles on a H-free support films [16–18].

The goal of the present study was to determine using simultaneous OA-STIM and Elastic Backscattering Spectrometry (EBS) the compositional changes in Pioloform films subject to realistic proton fluences used for trace element imaging by PIXE.

2. Experimental

Self-supporting Pioloform films with >97% purity were deposited according to Ren's protocol [19] in the My-fab cleanroom facility in Uppsala. The films were floated on the surface of Super-Q® water onto stainless steel M8 washers that supported the thin films.

Measurements were carried out using the MeV ion microprobe at the 5 MV Pelletron tandem accelerator in Uppsala [20]. The experimental configuration used for the measurements is shown in Fig. 2. The OA-STIM detector at 45° to the beam direction was a Hamamatsu S1223-01 Si pin diode with the cap removed and a 2.5 mm dia. collimator. The EBS detector was an annular Si surface barrier detector that detected ions at 168°. The charge collected in the Faraday cup was digitised with an Ortec 439 digitiser. Event-mode data collection was used with a FAST ComTec MPA-3 data collection system with 7072T ADCs. 120-mesh Ni and 1000-mesh Cu electron microscope grids were used to calibrate the scan sizes. The energy spectra were calibrated from edges for scattering from H, C, Al and Au reference samples.

* Corresponding author at: Department of Physics, University of Oslo, Postboks 1048 Blindern, Oslo, N-0316, Norway.
E-mail address: h.j.whitlow@fys.uio.no (H.J. Whitlow).

https://doi.org/10.1016/j.nimb.2023.03.028
Received 20 October 2022; Received in revised form 27 February 2023; Accepted 24 March 2023
Available online 10 April 2023

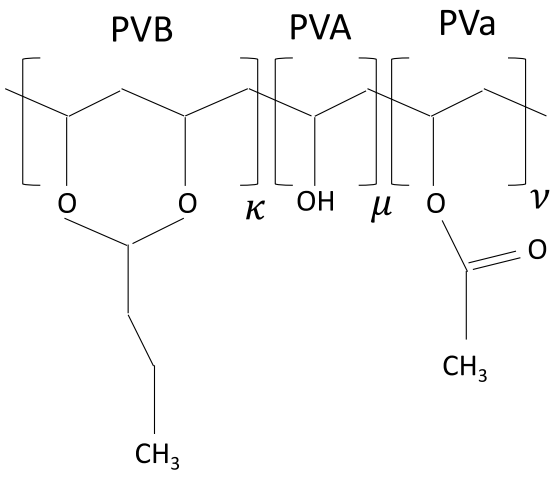

Fig. 1. Molecular structure of Pioloform. After: [7].

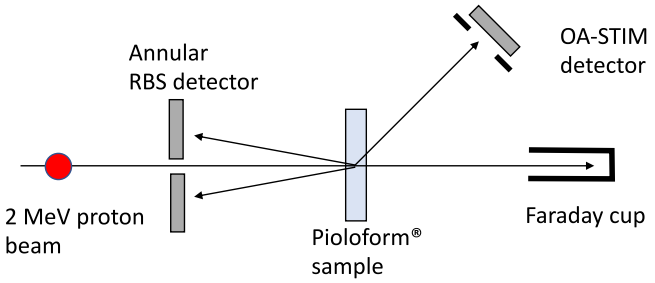

Fig. 2. Experimental measurement configuration in the target chamber.

Data was collected for 2 MeV protons focused to a ~3 μm beam spot that was rastered over a 100 μm × 100 μm area. The irradiations were performed step-wise for 100, 300, …, 10^4 s on the same area.

The GeoPIXE code was used to process the list-mode data file to extract the OA-STIM and EBS spectra for each fluence. In the EBS spectra a slowly varying background that was attributed to ions backscattered from the Faraday cup, was observed (Fig. 3(b)). The peak areas were determined after background subtraction.

3. Results and discussion

Fig. 3(a) and (b) presents the OA-STIM and EBS spectra from Pioloform film. The peaks in Fig. 3(a) correspond to recoiled C and O, a broad central peak from scattered and recoiled protons from p-p collisions and at high energy, peaks from protons forward-scattered at 45° from C and O.

Comparison of Fig. 3(a) and (b) showed that the peaks attributed to protons scattered from C and O in the EBS spectrum had a better energy separation than in the OA-STIM case. Moreover, the peak associated with scattered and recoiling protons from H was also well-isolated. A sensitivity factor η that relates the C peak yield $Y_{C_{EBS}}$ in the EBS spectra to the proton yield $Y_{H_{OAS}}$ in the OA-STIM spectra was defined.

$$\eta = \frac{\left(\frac{d\sigma_C}{d\Omega}\right)_{EBS}}{\left(\frac{d\sigma_{p-p}}{d\Omega}\right)_{OAS}} \cdot \frac{\Delta\Omega_{EBS}}{\Delta\Omega_{OA-STIM}} \tag{1}$$

The ratio of the solid-angle subtended by the EBS detector to that of the OA-STIM was determined from the yield ratio of protons scattered from carbon that were detected in the EBS $Y_{C_{EBS}}$ and OA-STIM $Y_{C_{OAS}}$ detectors.

$$\frac{\Delta\Omega_{EBS}}{\Delta\Omega_{OA-STIM}} = \frac{Y_{C_{EBS}}}{Y_{C_{OAS}}} \cdot \frac{\left(\frac{d\sigma_C}{d\Omega}\right)_{EBS}}{\left(\frac{d\sigma_C}{d\Omega}\right)_{OAS}} \tag{2}$$

In Eqs. (1) and (2) the differential scattering cross sections ($d\sigma/d\Omega$) are taken at 168° for C and 45° for H. It is well known that for light elements the differential cross-sections for elastic backscattering from light elements are non-Rutherford [21–24]. SigmaCalc [25,26] was used to calculate the differential cross-sections for backscattering from C and O. For the p–C and p–O OA-STIM signals, Elastic differential cross-sections were used since the energy available for barrier penetration is considerably smaller for forward scattering [27]. (The SigmaCalc [25,26] values differed by a few % and rather constant with energy around 2 MeV.) For p-p scattering in the OA-STIM spectra the $d\sigma_{p-p}/d\Omega$ cross sections were determined based on an empirical fit to the nuclear phase-shift that gave an excellent agreement with high-precision experimental $d\sigma_{p-p}/d\Omega$ data [27].

Fig. 4 shows the evolution of the composition of the Pioloform with proton fluence based on Eqs. (1) and (2). Considering first the low-fluence region ($\leq 10^{15}$ 2 MeV protons cm^{-2}) it was seen that the unirradiated (zero fluence) composition is in good agreement with the theoretical expectation for Pioloform (16 mass% PVA in PVB) [7]. It should be noted that since the yields were taken to be the area under the peaks associated with H (OA-STIM) as well as C and O (EBS), that the uncertainties were associated with counting statistics and not stopping cross-sections. Electronic screening effects were estimated based on Ref. [28] and found to be negligible. The C and O error bars were smaller than the data points in this figure. The O/C ratio is a very sensitive measurement of absorbed water due to e.g. hydrogen bonding. Based on its molecular structure (Fig. 1) PVB contains two singly bonded O atoms and could be expected to bond up to four H_2O molecules per PVB unit. Hydrogen bonding of one water molecule per PVB molecule would change the O/C ratio from 0.250 to 0.375. No significant increase of the zero-fluence O/C ratio was observed as can be deduced from the data of Fig. 4. Hence, no significant amount of water was contained in the polymer. It follows that Pioloform films can be used as an internal standard for H in simultaneous OA-STIM/EBS measurements with 1%–2% accuracy. This is provided that composition is extrapolated back to zero-fluence.

In Fig. 4 the normalised elemental contents are plotted. The increase in the normalised C content that was observed could be attributed to the greater net loss of H and O with increasing fluence. This was echoed in Fig. 5 where the retention of C, H and O is presented. An elemental retention of 100% corresponded to the composition in Fig. 4 extrapolated to zero fluence using a straight line fit to the two lowest fluence data points. It was found the elemental retention vs. fluence could not be fitted well by a function of the form $C = A + B\exp(-\lambda\Theta)$ (Fig. 5). Such a function corresponds to a single loss process with a constant retained value. Generally, irradiated polymers tend to release small molecules [29] such as H_2, CH_4, CO, CO_2 and H_2O etc. as well as larger fragments such as pendant side-chains. Fig. 1 showed that there are multiple sites where irradiation induced bond breaking could lead to release of small molecular fragments through bond scission as well as abstraction reactions.

4. Conclusions

Off-axis Scanning Transmission Ion Microscopy (STIM) and Elastic backscattering spectrometry (EBS) have been successfully employed to characterise the content of C, H and O in Pioloform films. The zero-fluence composition corresponded very closely to the theoretical expectation with no evidence of significant water incorporation associated with hydrogen bonding. This facilitates use as an internal standard provided the composition is extrapolated back to zero-fluence. A proton fluence dependent composition change was observed. With increasing proton fluence H and O was preferentially lost compared to C, at rates consistent with multiple loss mechanisms.

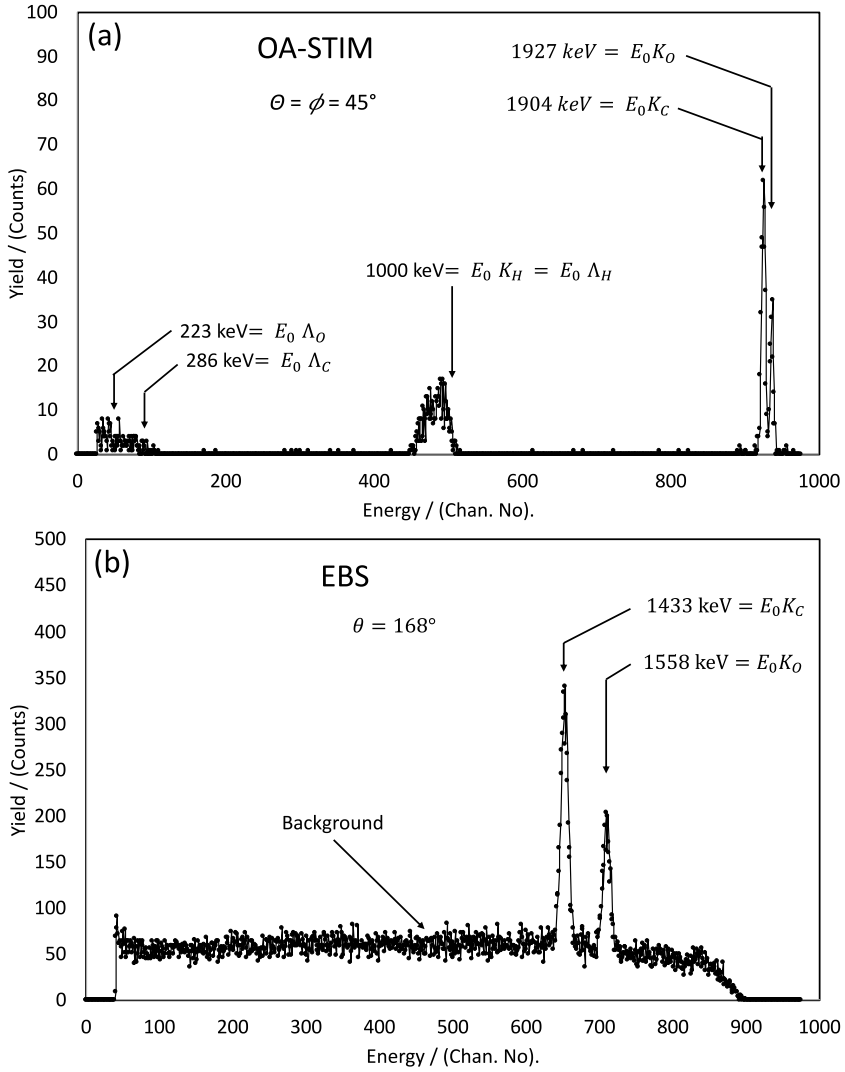

Fig. 3. (a) OA-STIM and (b) EBS energy spectra from Pioloform film.

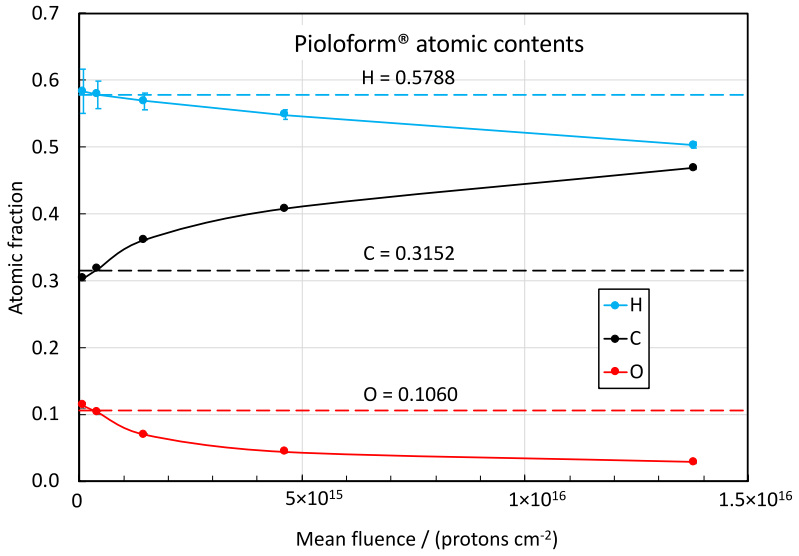

Fig. 4. Fluence dependence of the normalised atomic composition of Pioloform for a 2 MeV proton irradiation. The dashed lines denote the theoretical composition of PVB with 16 mass % PVA [7].

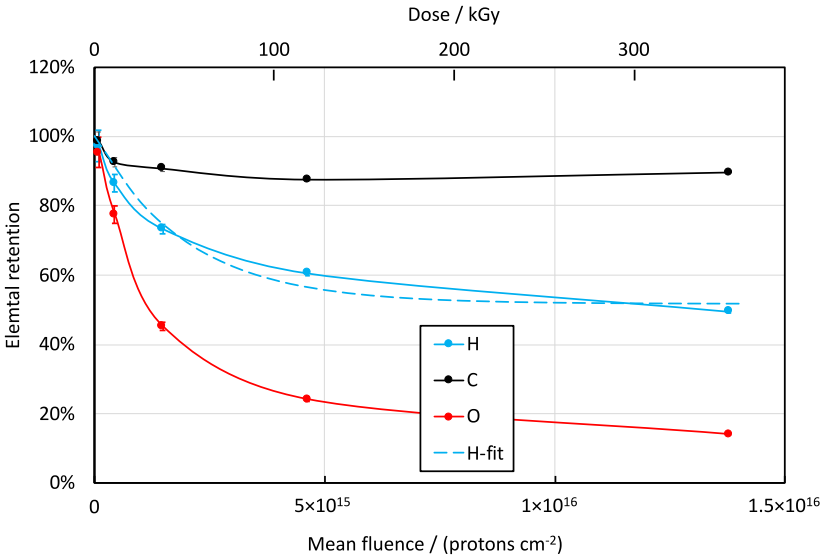

Fig. 5. Fluence dependence of the retained content of C, H and O at a proton energy of 2 MeV. The dashed blue line shows the best fit to a single exponential loss. (See text.).

Declaration of competing interest

The authors declare that they have no known competing financial interests or personal relationships that could have appeared to influence the work reported in this paper.

Acknowledgements

Accelerator operation is supported by the Swedish Research Council VR-RFI (Contracts No. 2017-00646_9 and 2019-00191) and the Swedish Foundation for Strategic Research (Contract No. RIF14-0053). We acknowledge Myfab Uppsala for providing facilities and experimental support. Myfab is funded by the Swedish Research Council (2019-00207) as a national research infrastructure. HJW acknowledges support from The Research Council of Norway for the Norwegian Micro and Nano-Fabrication Facility, NorFab (Project 11 No. 245963.)

References

[1] M. Ren, J. Xie, X. Wang, W. Ong, S. Leong, F. Watt, Iron concentrations and distributions in the parkinsonian substantia nigra of aged and young primate models, Nucl. Instrum. Methods Phys. Res. B 181 (1) (2001) 522–528, http://dx.doi.org/10.1016/S0168-583X(01)00482-7, 7th International Conference on Nuclear Microprobe Technology and Applications. URL https://www.sciencedirect.com/science/article/pii/S0168583X01004827.

[2] M.-Q. Ren, W.-Y. Ong, X.-S. Wang, F. Watt, A nuclear microscopic and histochemical study of iron concentrations and distribution in the midbrain of two age groups of monkeys unilaterally injected with MPTP, Exp. Neurol. 184 (2) (2003) 947–954, http://dx.doi.org/10.1016/S0014-4886(03)00341-8, URL https://www.sciencedirect.com/science/article/pii/S0014488603003418.

[3] R. Minqin, F. Watt, B. Tan Kwong Huat, B. Halliwell, Trace elemental distributions in induced atherosclerotic lesions using nuclear microscopy, Nucl. Instrum. Methods Phys. Res. B 210 (2003) 336–342, http://dx.doi.org/10.1016/S0168-583X(03)01062-0, 8th International Conference of Nuclear Microprobe Technology and Applications. URL https://www.sciencedirect.com/science/article/pii/S0168583X03010620.

[4] H.J. Whitlow, M. Ren, J.A. van Kan, F. Watt, D. White, Exploratory nuclear microprobe data visualisation using 3- and 4-dimensional biological volume rendering tools, Nucl. Instrum. Methods Phys. Res. B 260 (1) (2007) 28–33, http://dx.doi.org/10.1016/j.nimb.2007.01.316, Nuclear Microprobe Technology and Applications (ICNMTA2006) and Proton Beam Writing (PBW II). URL https://www.sciencedirect.com/science/article/pii/S0168583X07003357.

[5] H.J. Whitlow, N.T. Deoli, A. de Vera, K. Morgan, F. Villinger, Heavy elements revealed in jejunum of simian immunodeficiency virus infected monkeys by microparticle induced X-Ray emission, Phys. Status Solidi (A) 218 (1) (2021) 2000107, http://dx.doi.org/10.1002/pssa.202000107, URL https://onlinelibrary.wiley.com/doi/abs/10.1002/pssa.202000107.

[6] H.J. Whitlow, N. Henderson, R. Greco, N. Deoli, K.M. Smith, K. Morgan, F. Villinger, PIXE studies of normal and SIV-infected rhesus macaque tissues: investigations of particulate matter, J. Phys.: Conf. Ser. 2326 (2022) 012010, http://dx.doi.org/10.1088/1742-6596/2326/1/012010.

[7] C. Carrot, A. Bendaoud, C. Pillon, Handbook of Thermoplastics, CRC Press, 2015, http://dx.doi.org/10.1201/b19190-4, Ch. 3, Polyvinyl Butyral. URL https://www.routledgehandbooks.com/doi/10.1201/b19190-4.

[8] R. Norarat, V. Marjomäki, X. Chen, M. Zhaohong, R. Minqin, C.-B. Chen, A. Bettiol, H. Whitlow, F. Watt, Ion-induced fluorescence imaging of endosomes, Nucl. Instrum. Methods Phys. Res. B 306 (2013) 113–116, http://dx.doi.org/10.1016/j.nimb.2012.12.052, 13th International Conference on Microprobe Technology and Applications (ICNMTA2012). URL https://www.sciencedirect.com/science/article/pii/S0168583X13000281.

[9] R. Minqin, J. van Kan, A. Bettiol, L. Daina, C.Y. Gek, B.B. Huat, H. Whitlow, T. Osipowicz, F. Watt, Nano-imaging of single cells using STIM, Nucl. Instrum. Methods Phys. Res. B 260 (1) (2007) 124–129, http://dx.doi.org/10.1016/j.nimb.2007.02.015, Nuclear Microprobe Technology and Applications (ICNMTA2006) and Proton Beam Writing (PBW II). URL https://www.sciencedirect.com/science/article/pii/S0168583X07003539.

[10] J. Pallon, C. Ryan, N. Arteaga Marrero, M. Elfman, P. Kristiansson, E. Nilsson, C. Nilsson, STIM evaluation in GeoPIXE to complement the quantitative dynamic analysis, Nucl. Instrum. Methods Phys. Res. B 267 (12) (2009) 2080–2084, http://dx.doi.org/10.1016/j.nimb.2009.03.036, Proceedings of the 11th International Conference on Nuclear Microprobe Technology and Applications and the 3rd International Workshop on Proton Beam Writing. URL https://www.sciencedirect.com/science/article/pii/S0168583X09003486.

[11] P. Aguer, L. Alves, P. Barberet, E. Gontier, S. Incerti, C. Michelet-Habchi, Z. Kertész, A. Kiss, P. Moretto, J. Pallon, T. Pinheiro, J. Surlève-Bazeille, Z. Szikszai, A. Veríssimo, M. Ynsa, Skin morphology and layer identification using different STIM geometries, Nucl. Instrum. Methods Phys. Res. B 231 (1) (2005) 292–299, http://dx.doi.org/10.1016/j.nimb.2005.01.073, Nuclear Microprobe Technology and Applications. URL https://www.sciencedirect.com/science/article/pii/S0168583X05000935.

[12] T. Kaniya, T. Sakai, M. Oikawa, T. Satoh, K. Ishii, A. Sugimoto, S. Matsuyama, STIM imaging of mammalian cell samples before micro-PIXE analysis in air envirommentat at JAERI light ion microprobe system, Int. J. PIXE 09 (03n04) (1999) 217–225, http://dx.doi.org/10.1142/S0129083599000310.

[13] K. Inomata, K. Ishii, H. Yamazaki, S. Matsuyama, Y. Kikuchi, Y. Watanabe, A. Ishizaki, R. Oyama, Y. Kawamura, T. Yamaguchi, G. Momose, E. Sakurai, K. Yanai, T. Kamiya, T. Sakai, T. Satoh, M. Oikawa, K. Arakawa, Development of an in-air on/off axis STIM system for quantitative elemental mapping, Int. J. PIXE 16 (2006) 149–156, http://dx.doi.org/10.1142/S0129083506000939.

[14] K. Sjöland, P. Kristiansson, Off-axis STIM nuclear microprobe analysis, Nucl. Instrum. Methods Phys. Res. B 118 (1) (1996) 451–455, http://dx.doi.org/10.1016/0168-583X(95)01093-9, Ion Beam Analysis. URL https://www.sciencedirect.com/science/article/pii/0168583X95010939.

[15] J. Pallon, V. Auzelyte, M. Elfman, M. Garmer, P. Kristiansson, K. Malmqvist, C. Nilsson, A. Shariff, M. Wegdén, An off-axis STIM procedure for precise mass determination and imaging, Nucl. Instrum. Methods Phys. Res. B 219–220 (2004) 988–993, http://dx.doi.org/10.1016/j.nimb.2004.01.201, Proceedings of the Sixteenth International Conference on Ion Beam Analysis. URL https://www.sciencedirect.com/science/article/pii/S0168583X04002514.

[16] G. Bench, P.G. Grant, D. Ueda, S.S. Cliff, K.D. Perry, T.A. Cahill, The use of STIM and PESA to measure profiles of aerosol mass and hydrogen content, respectively, across mylar rotating drums impactor samples, Aerosol Sci. Technol. 36 (5) (2002) 642–651, http://dx.doi.org/10.1080/02786820252883874, arXiv: https://doi.org/10.1080/02786820252883874.

[17] M. Chiari, G. Calzolai, M. Giannoni, F. Lucarelli, S. Nava, S. Becagli, Use of proton elastic scattering techniques to determine carbonaceous fractions in atmospheric aerosols collected on Teflon filters, J. Aerosol Sci. 89 (2015) 85–95, http://dx.doi.org/10.1016/j.jaerosci.2015.07.006, URL https://www.sciencedirect.com/science/article/pii/S0021850215001123.

[18] J. Voltr, J. Král, Z. Nejedlý, PESA as a complementary tool to PIXE at CTU Prague, Nucl. Instrum. Methods Phys. Res. B 150 (1) (1999) 554–558, http://dx.doi.org/10.1016/S0168-583X(98)00951-3, URL https://www.sciencedirect.com/science/article/pii/S0168583X98009513.

[19] M.-Q. Ren, Nuclear Microscopy: Development and applicatiosn in Atheroschlerosis, Parkinsons Disease and Materials Physics (Ph.D. thesis), Faculty of Mathematics and Natural Sciences, Jyväskylä, Finland, 2007.

[20] G. Nagy, H.J. Whitlow, D. Primetzhofer, The scanning light ion microprobe in Uppsala – Status in 2022, Nucl. Instrum. Methods Phys. Res. B 533 (2022) 66–69, http://dx.doi.org/10.1016/j.nimb.2022.10.017, URL https://www.sciencedirect.com/science/article/pii/S0168583X22003007.

[21] A. Gurbich, Evaluation of non-Rutherford proton elastic scattering cross section for carbon, Nucl. Instrum. Methods Phys. Res. B 136–138 (1998) 60–65, http://dx.doi.org/10.1016/S0168-583X(97)00837-9, Ion Beam Analysis. URL https://www.sciencedirect.com/science/article/pii/S0168583X97008379.

[22] K. Gul, K. Shahzad, J. Taj, A. Awais, J. Hussain, F. Qureshi, N. Ali, Experimental study of proton scattering on carbon, Nucl. Instrum. Methods Phys. Res. B 269 (18) (2011) 2032–2034, http://dx.doi.org/10.1016/j.nimb.2011.06.006, URL https://www.sciencedirect.com/science/article/pii/S0168583X1100591X.

[23] A. Gurbich, Evaluation of non-Rutherford proton elastic scattering cross section for nitrogen, Nucl. Instrum. Methods Phys. Res. B 266 (8) (2008) 1193–1197, http://dx.doi.org/10.1016/j.nimb.2007.11.026, Ion Beam Analysis. URL https://www.sciencedirect.com/science/article/pii/S0168583X07017235.

[24] A. Gurbich, Evaluation of non-Rutherford proton elastic scattering cross section for oxygen, Nucl. Instrum. Methods Phys. Res. B 129 (3) (1997) 311–316, http://dx.doi.org/10.1016/S0168-583X(97)00288-7, URL https://www.sciencedirect.com/science/article/pii/S0168583X97002887.

[25] A. Gurbich, SigmaCalc recent development and present status of the evaluated cross-sections for IBA, Nucl. Instrum. Methods Phys. Res. B 371 (2016) 27–32, http://dx.doi.org/10.1016/j.nimb.2015.09.035, The 22nd International Conference on Ion Beam Analysis (IBA 2015). URL https://www.sciencedirect.com/science/article/pii/S0168583X15008940.

[26] A. Gurbich, SigmaCalc, 2015, URL http://sigmacalc.iate.obninsk.ru.

[27] H.J. Whitlow, On quantitative off-axis scanning transmission ion microscopy (STIM), Nucl. Instrum. Methods B - Accepted for publication (2022) Acccepted.

[28] H.H. Andersen, F. Besenbacher, P. Loftager, W. Möller, Large-angle scattering of light ions in the weakly screened Rutherford region, Phys. Rev. A 21 (1980) 1891–1901, http://dx.doi.org/10.1103/PhysRevA.21.1891, URL https://link.aps.org/doi/10.1103/PhysRevA.21.1891.

[29] A. Chapiro, Chemical modifications in irradiated polymers, Nucl. Instrum. Methods Phys. Res. B 32 (1) (1988) 111–114, http://dx.doi.org/10.1016/0168-583X(88)90191-7, URL https://www.sciencedirect.com/science/article/pii/0168583X88901917.